

Optimization and Intelligence Modelling of Residual Stresses in Mild Steel Plate Weldments Obtained Using Gas Tungsten Arc Welding Process

M.K. Achike^{1*}, P. C. Onyechi² and C. C. Ihueze³

^{1*}Department of Metalwork Technology Education, Federal College of Education (Technical), Umunze, Nigeria.

^{2,3}Department of Industrial/Production Engineering, Nnamdi Azikiwe University, Awka, Nigeria.
Corresponding Author: achike4christ07@yahoo.com

Abstract

This paper aimed at optimizing the process parameters and intelligence modelling of residual stresses in mild steel plate weldments obtained using Gas Tungsten Arc Welding (GTAW) process. Taguchi robust design and intelligent modeling techniques (artificial neural networks and extreme learning machine) were used to model the experimental results. In designing the experimental runs for this research, Taguchi design of experiment which consists of four controllable parameters at 3-levels of design for which we chose the L_9 orthogonal array was used. Signal-to-noise ratio (S/N) which is an important quality characteristics of Taguchi method employed the smaller-the-better criterion for residual stress response. Minitab 16 Software was used for analysis of signal-to-noise ratio and ANOVA was used to validate the results at 95% confidence level. The ANN and ELM model simulations were carried out in MATLAB 2018a environment at three different hidden neural nodes of 10, 20 and 30 neurons for thirty (30) experimental runs. ELM model showed a very good model fit at 30 neural nodes with a coefficient of determination (R^2) value of 99.2% which is far better than that of ANN and regression models which has R^2 values of 96.5% and 92.4% respectively. By comparing the experimental results with those obtained using ANN and ELM models, it can be concluded that the ELM model is more efficient in predicting residual stress in mild steel plate weldments.

Keywords: Gas Tungsten Arc Welding, Residual Stress, Taguchi Method, ANN, ELM

Date of Submission: 23-08-2021

Date of acceptance: 07-09-2021

I. Introduction

Welding is one of the most important technologies widely used in various engineering fields such as civil engineering, shipbuilding, pipeline fabrication, steel structural fabrication among others. It is a complicated process accompanied by shrinkage effects, phase transformations, intensification of corrosion and arising of residual stresses. The American Welding Society (2004) defined welding as a localized coalescence of metals or non-metals produced by either heating of the materials to a suitable temperature with or without the application of pressure, or by the application of pressure alone with or without the use of a filler material. It is a process that involves localized heat generation from a moving heat source. The welded structures are heated rapidly up to the melting temperature, and followed by rapid cooling which cause's micro-structural and property alteration. Arc welding processes use a welding power supply to create and maintain an electric arc between an electrode and the base material to melt metals at the welding point.

Many distinct factors influence the strength of welds and the material around them, including the welding method, the amount and concentration of energy input, the weldability of the base material, filler material, and flux material, the design of the joint, and the interactions between all these factors. To test the quality of a weld, either destructive or nondestructive testing methods are commonly used to verify that welds are free of defects, have acceptable levels of residual stresses and distortion, and have acceptable heat-affected zone (HAZ) properties.

Withers and Bhadeshia (2001) identify residual stress as the stress that remain within a material or body after manufacture and material processing in the absence of external forces or thermal gradients. Welding is one of the most significant causes of residual stresses and typically produces large tensile stresses in the weld, balanced by lower compressive residual stresses elsewhere in the component. Tensile residual stresses may reduce the performance or cause failure of manufactured products. They may increase the rate of damage by fatigue, creep or environmental degradation. They may reduce the load carrying capacity of a component by

contributing to failure by brittle fracture, or cause other forms of damage such as shape change or crazing (Bate, Green and Buttle, 1997; Masubichi, 1980).

Gas Tungsten Arc Welding (GTAW) uses a non-consumable tungsten electrode to heat and melt the workpiece and a separate filler metal with an inert shielding gas to protect the arc. A GTAW process set utilizes suitable power source, a cylinder of inert gas, a welding torch having connections of cable for current, tubing for shielding gas supply, and tubing for water for cooling the torch. The shape of torch is characteristic, having a cap at the back end to protect the rather long tungsten electrodes against accidental breakage. Filler metal can be fed and molten puddle is shielded from the atmosphere with an inert gas supply feeding from the torch cup (Jain, 2013).

Design of Experiment (DOE): Taguchi Approach

The modern day approach to find the optimal output over a set of given inputs can be easily carried out by the use of Taguchi method rather than using any other conventional method. The Taguchi method emphasizes the selection of the most optimal solution over the set of given inputs with a reduced cost and increased quality. The optimal solution so obtained is least affected by any outside disturbances like the noise or any other environmental conditions (Rao *et al*, 2008). Okafor, Ihueze and Nwigbo (2013) viewed Taguchi robust design as a method of designing experiments in order to investigate how different parameters affect the mean and variance of a process performance characteristic that define how well the process is functioning. The Taguchi method emphasizes the use of loss function, which is the deviation from the desired value of the quality characteristics. Based on loss function, the Signal-to-Noise ratio for each experimental set is evaluated and accordingly the optimal results are derived. For residual stress response, S/N ratio is based upon the smaller-the-better criterion which is calculated using equation 1.

$$\frac{S}{N} = -10 \log \frac{1}{n} \left(\sum y_i^2 \right) \tag{1}$$

Where n = number of measurements,

y_i = response value for each measurement.

In order to optimize residual stress response, four process parameters (current I, voltage V, welding speed S and plate thickness t) were considered. Equally spaced three levels within the operating range of the process parameters were selected as presented in table 1. Based on Taguchi method, an L₉ (3⁴) Orthogonal Array (OA) which has nine different experiments was conducted and the result is shown in table 4.

Table 1: Process Parameters, Codes, and Level values

Process Parameter	Code	Levels		
		1	2	3
Welding Current (A)	I	100	130	160
Welding Voltage (V)	V	24	28	32
Welding Speed (mm/min)	S	90	120	150
Plate Thickness (mm)	t	6	8	10

Sample Production

For each weldment, two plates of dimension 300×120×10mm, 300x120x8mm, and 300x120x6mm in each case were cut and welded to make a weld specimen plate of 300×240×10mm, 300×240×8mm, and 300×240×6mm respectively with a 300 mm weld length. Prior to welding, the plates were cleaned from water, dust and oil to enable proper deposition of electrodes. 60° V-groove was cut by abrasive cutting on one side of the plates and the plates were tack-welded at both ends in order to eliminate distortion during welding. All necessary precautions were taken to eliminate welding defects. The 60° V-groove butt joint was made employing symmetric welding sequence as shown in figure 1. Table 2 show the welding consumables and machine settings used during welding.

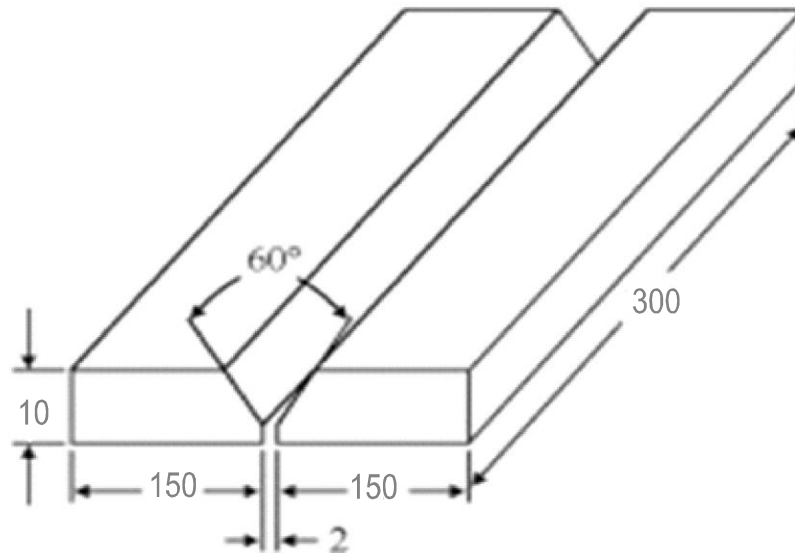


Figure 1: Plate set-up prior to welding

Table 2: GTAW Parameters

S/N	Parameter	6mm plate	8mm plate	10mm plate
1	Electrode type	2% Thoriated W (red) 2.0mm	2% Thoriated W (red) 2.5mm	2% Thoriated W (red) 3.0mm
2	Filler rod	Mild steel 2.0mm	Mild steel 2.5mm	Mild steel 3.0mm
3	Included angle	60°	60°	60°
4	Root face	1.0mm	1.5mm	2.0mm
5	Root gap	1.0mm	1.2mm	1.5mm
6	Gas flow rate	5l/min	7.5l/min	10l/min
7	Current (A)	100, 130, 160	100, 130, 160	100, 130, 160
8	Voltage (V)	24, 28, 32	24, 28, 32	24, 28, 32
9	Number of runs	3	3	3
10	Shielding gas	Helium	Helium	Helium

Residual Stress Measurement

X-ray diffraction (XRD) is a well-established, non-destructive method for the determination of residual stress in polycrystalline materials. 75% of companies and academics prefer to use XRD method in measuring residual stresses because the method is fast, can be repeatable, harmless to the specimen, and can control the specimen quality (Mazzolani, 2005). Residual stress induces small changes in the crystal lattice spacing of a material, which can be revealed by XRD with a very high sensitivity. From this, the lattice spacing in different directions and the related elastic strain can be determined. X-Ray Diffraction (XRD) was carried out on each of the samples in order to calculate the residual stress induced during welding. The ψ angles were tilted in steps of 9° in the range of 0° to 45°. The residual stress was estimated using the peak shift at ψ angles and d-spacing relationship of (211) plane. The Young modulus (E) and Poisson's ratio (ν) of mild steel was taken as 210 GPa and 0.290 respectively in order to estimate the residual stress values. The residual stress (σ) was calculated by using equations (2) and (3) as derived by Cullity and Stock (2001) :

$$\varepsilon = \frac{d - d_o}{d_o} \tag{2}$$

$$\sigma = \frac{E}{1 + \nu} \times \frac{1}{\sin^2 \psi} \times \varepsilon \tag{3}$$

Where d_o is the strain free inter planer spacing, ε is the calculated strain and angle ψ is the angle between the surface normal and strain measurement direction. The change in inter planer space "d" due to residual stress was measured from XRD graphics as shown in figure 2 and tabulated in table 3.

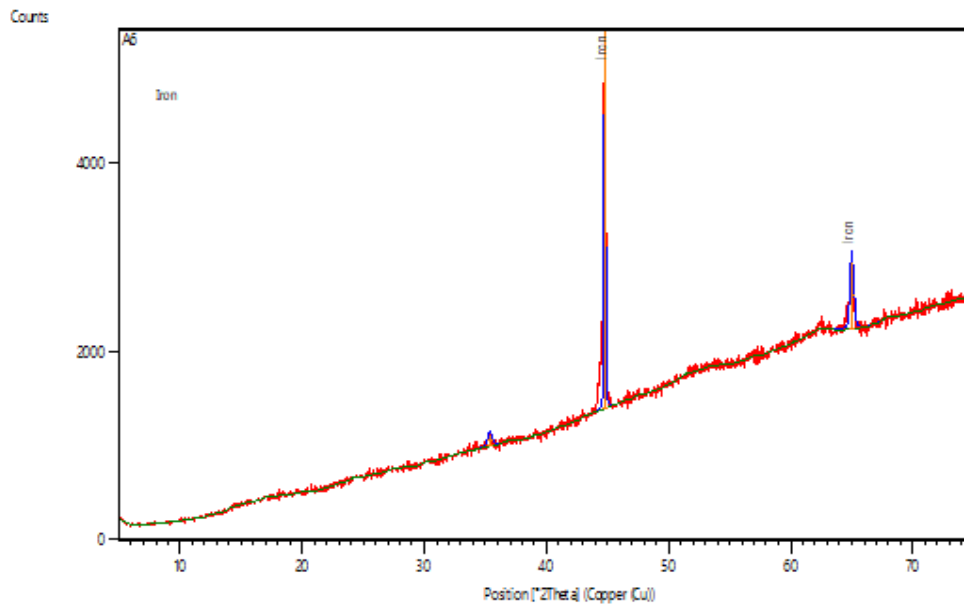


Figure 1: XRD Graphics

Table 3: Peak List

Pos.[°2Th.]	Height [cts]	FWHMLeft[°2Th.]	d-spacing [Å]	Rel. Int. [%]
35.3346	115.99	0.4093	2.54024	2.83
38.7350	204.21	0.0768	2.02587	10.00
44.9595	215.44	0.2558	1.43563	17.43
49.8367	99.08	0.6140	2.50580	14.69
55.2773	213.18	0.1279	2.00286	12.00
63.0348	181.53	0.6140	1.47475	8.59
65.4184	249.20	0.6140	1.42667	11.79
67.2773	113.18	0.1279	2.00286	16.24
68.0348	161.53	0.6140	1.47475	18.59

II. Experimental Results

The experimental result of residual stress (Table 4) was analyzed using Taguchi robust design. Minitab16 software was used for the Taguchi analysis which yielded the regression model for predicting residual stress response. The response tables for signal-to-noise ratio and means (Table 5 and Table 6) for levels of each factor was obtained. The ranks based on delta statistics which compare the relative magnitude of effects were also analyzed.

Table 4: Residual Stress Response for GTAW

S/N	Input Parameters				Residual Stress (MPa)
	Current (I) A	Voltage (V) V	Welding Speed (S) mm/min	Plate Thickness (t) mm	
1	100	24	90	6	125.8
2	100	28	120	8	90.5
3	100	32	150	10	82.0
4	130	24	120	10	108.6
5	130	28	150	6	96.6
6	130	32	90	8	158.6
7	160	24	150	8	102.5
8	160	28	90	10	165.4
9	160	32	120	6	152.0

Table 5: Response Table for Signal to Noise Ratio

	Current	Voltage	Welding Speed	Plate Thickness
Level	(A)	(V)	(mm/min)	(mm)
1	-39.80	-40.97	-43.46	-41.78
2	-41.47	-41.07	-41.16	-41.12
3	-42.74	-41.97	-39.40	-41.12
Delta	2.94	1.00	4.06	0.66
Rank	2	3	1	4

Table 6: Response Table for Means

	Current	Voltage	Welding Speed	Plate Thickness
Level	(A)	(V)	(mm/min)	(mm)
1	99.43	112.30	149.93	124.80
2	121.27	117.50	117.03	117.20
3	139.97	130.87	93.70	118.67
Delta	40.53	18.57	56.23	7.60
Rank	2	3	1	4

Table 7: Analysis of Variance for SN Ratio

Source	DF	Seq SS	Adj SS	Adj MS	F	P
Current (A)	2	13.0457	13.0457	6.5228	1.55	0.215
Voltage (V)	2	1.8246	1.8246	0.9123	0.24	0.055
Welding Speed (mm/min)	2	24.8658	24.8658	12.4329	2.42	0.342
Plate Thickness (mm)	2	0.8637	0.8637	0.4319	0.08	0.000
Residual Error	0	0.0000				
Total	8	40.5998				

S = 1.7530 R² = 92.4% R² (Adj) = 38.6%

Table 8: Analysis of Variance for Means

Source	DF	Seq SS	Adj SS	Adj MS	F	P
Current (A)	2	2469.34	2469.34	1234.67	28.43	0.308
Voltage (V)	2	550.43	550.43	275.21	9.26	0.254
Welding Speed (mm/min)	2	4789.04	4789.04	2394.52	36.84	0.421
Plate Thickness (mm)	2	97.53	97.53	48.76	3.75	0.020
Residual Error	0	0.00				
Total	8	7906.34				

S = 22.8482 R² = 92.2% R² (Adj) = 38.2%

The estimated model for S/N ratio is obtained as:

$$y = -41.3386 + 1.5376I - 0.1355I + 0.3637V + 0.2708V - 2.1182S + 0.1764S - 0.4381t + 0.2207t \tag{4}$$

The estimated model for Means is obtained as:

$$y = 120.222 - 20.789I + 1.044I - 7.922V - 2.722V + 29.711S - 3.189S + 4.578t - 3.022t \tag{5}$$

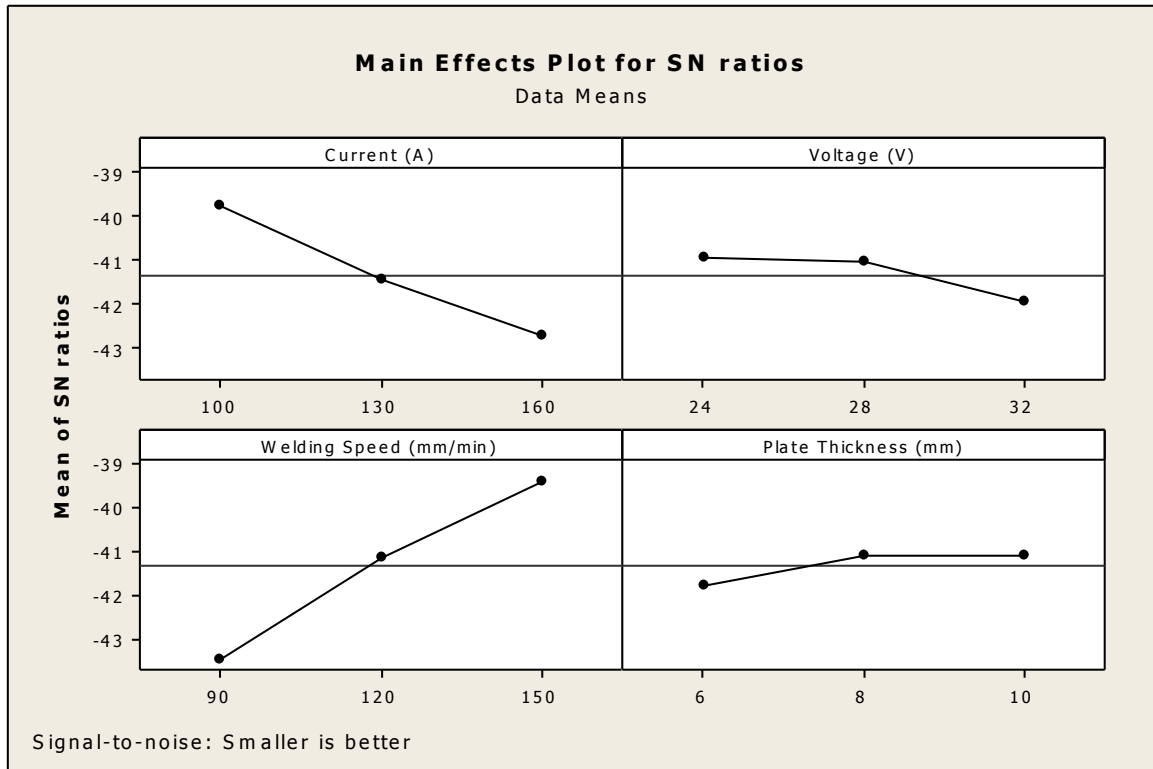


Figure 3: Main Effects Plot for SN Ratio

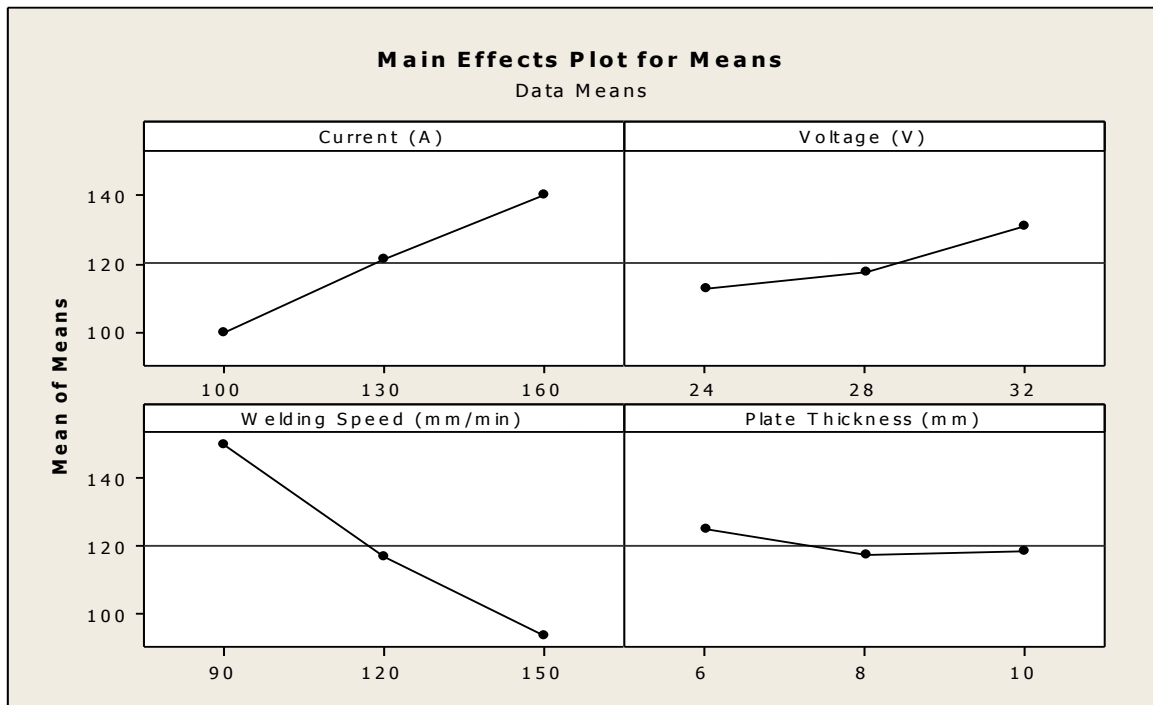


Figure 4: Main Effects Plot for Means

Interpreting the Result of Residual Stress Response for GTAW Process

The response tables for signal-to-noise ratio and means for levels of each factor are shown in table 5 and table 6. The ranks in these response tables indicate that welding speed has the greatest influence on residual stress response of mild steel plate weldments obtained using gas tungsten arc welding process. This was followed by welding current, welding voltage and plate thickness respectively.

In the analysis of variance, the coefficient of determination (R^2) at this point was 92.4% and 92.2% for S/N ratio and mean respectively. This indicates that the linear models of S/N ratio and mean were able to show

92.4% and 92.2% of the variation observed in the dependent variable as captured by the explanatory variables in the linear regression model. These models were completely linear; they did not show interaction effects of the variables.

The main effects plots for S/N ratio and that of means (Figs. 3 and 4) respectively indicate the same outcome of optimum. They show that the optimal residual stress for gas tungsten arc welding was achieved at a welding current of 100A, welding voltage of 32V, welding speed of 150mm/min and plate thickness of 10mm.

The main effect plots, ranks of factors, values of sum of squares from ANOVA tables are all in conformity with coefficients of the linear models produced for this response. The absolute value of these coefficients shows the importance of each factor to the response; hence, welding speed remains the most significant factor. Based on equations (4) and (5), the optimal residual stress was obtained as 76MPa and 84MPa for S/N ratio and for means respectively.

Intelligence Modelling

The machine learning algorithms applied in this research are artificial neural networks (ANN) and extreme learning machine (ELM) which are both feed-forward neural networks. The ANN and ELM model simulations were carried out in MATLAB 2018a environment at three different hidden neural nodes of 10, 20 and 30 neurons for the thirty (30) experimental runs. The optimum ELM model was determined using the Sigmoid hidden transfer function while the optimum ANN model was determined using Levenberg-Marquart back propagation training algorithm.

The original dataset was split into training, cross-validation and test data sets, where;

- 70% of the exemplars were presented to the network for training.
- 15% of the exemplars concurrent with the training set were used for cross validation.
- 15% of the exemplars were used for testing the trained network.

The following termination criteria were used to determine convergence of the training algorithm:

- Number of runs before termination.
- Maximum number of runs.
- Non-improvement of cross-validation error with training.
- Increase in the cross-validation error with training.

Furthermore, a performance comparison in terms of estimation capacity was conducted between the two models to show their potential in predicting the response.

Score Metrics for ANN and ELM Models

To validate and compare the results from ANN and ELM models, the following score metrics were statistically evaluated. They are; Mean Square Error (MSE), Root Mean Square Error (RMSE), Mean Absolute Deviation (MAD), Mean Absolute Percentage Error (MAPE), Tracking Signal (TS) (Narasimhan, Mcleavey, and Billington, 1995; Vonderembse and White, 1991) and Coefficient of Determination (R^2) (Thorstom, 2017). These score metrics are expressed as follows;

$$MSE = \frac{1}{N} \sum_{i=1}^n (R_{Pi} - R_{Ti})^2 \tag{6}$$

$$RMSE = \sqrt{\frac{1}{N} \sum_{i=1}^n (R_{Pi} - R_{Ti})^2} \tag{7}$$

$$MAD = \frac{1}{N} \sum_{i=1}^n |(R_{Ti} - R_{Pi})| \tag{8}$$

$$MAPE = \frac{\sum (|R_T - R_P| / R_T) * 100}{N} \tag{9}$$

$$TS = \frac{\sum_{i=1}^n \frac{R_{Ti} - R_{Pi}}{R_{Ti}}}{\frac{1}{N} \sum_{i=1}^n |(R_{Ti} - R_{Pi})|} \tag{10}$$

$$R^2 = 1 - \frac{\sum_{i=0}^{n_{samples}-1} (R_{Ti} - R_{Pi})^2}{\sum_{i=0}^{n_{samples}-1} (R_{Ti} - \bar{R})^2} \tag{11}$$

where R_{Pi} and R_{Ti} are the predicted and the targeted responses.

ANN and ELM Prediction Results at 10, 20 and 30 Nodes

The ANN and ELM simulation results alongside the experimental results at 10 nodes, 20 nodes and 30 nodes are presented in Tables 9 for Residual stress response.

Table 9: Residual Stress Prediction for GTAW

Experimental	ANN			ELM		
	10 Nodes	20 Nodes	30 Nodes	10 Nodes	20 Nodes	30 Nodes
96.6	161.74905	123.28795	116.72308	107.87378	106.32759	122.711
165.4	193.68187	220.91094	184.11053	189.13412	178.26355	203.05923
125.8	133.08782	129.88185	142.76185	139.0696	133.61222	169.13763
102.5	128.22054	154.33782	137.53861	131.16396	107.14772	148.81538
90.5	151.28759	93.00252	99.82218	110.88539	100.64527	121.2947

Prediction Comparison of Residual Stress at 10, 20 and 30 Nodes

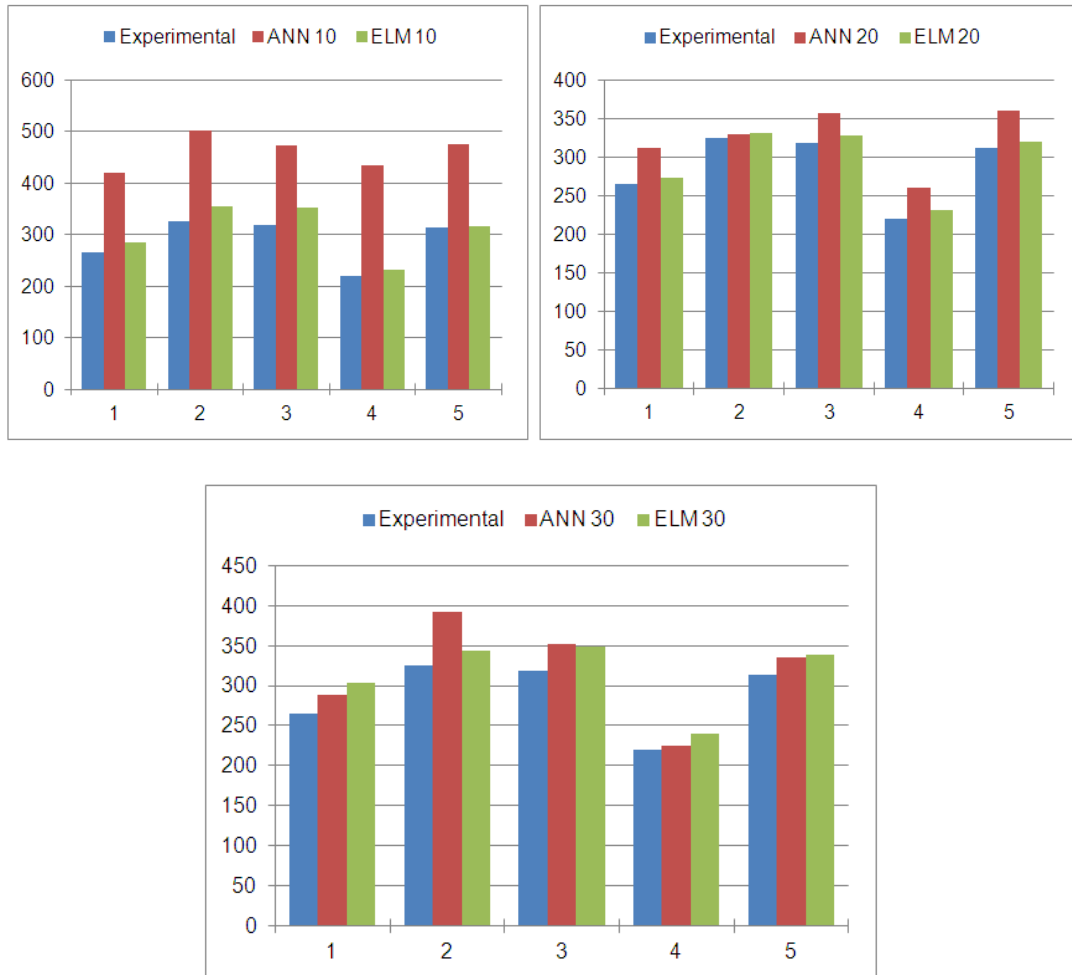
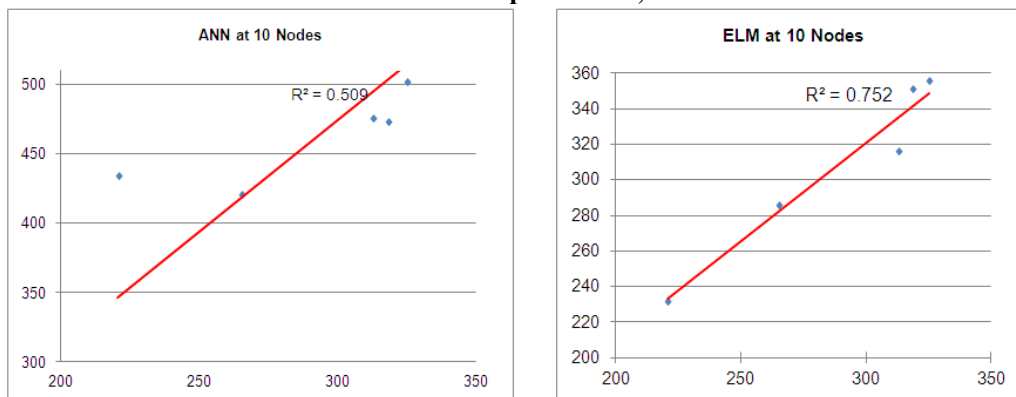


Figure 5: ANN and ELM Prediction Comparison of Residual Stress at 10, 20 and 30 Nodes

ANN and ELM Scatter Plots for Residual Stress Response at 10, 20 and 30 Nodes



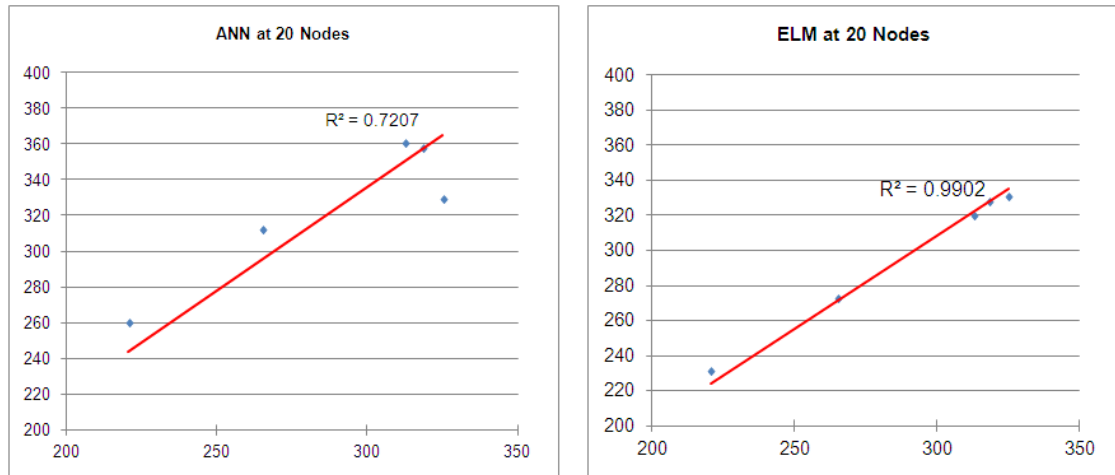


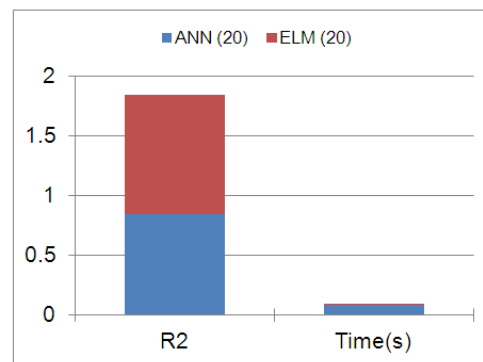
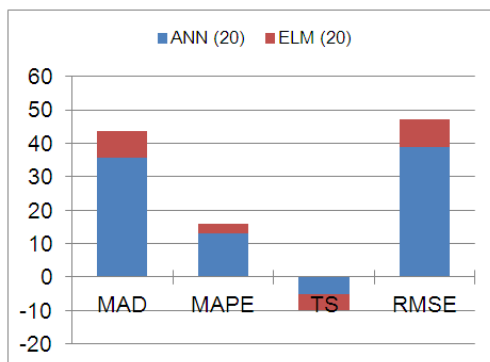
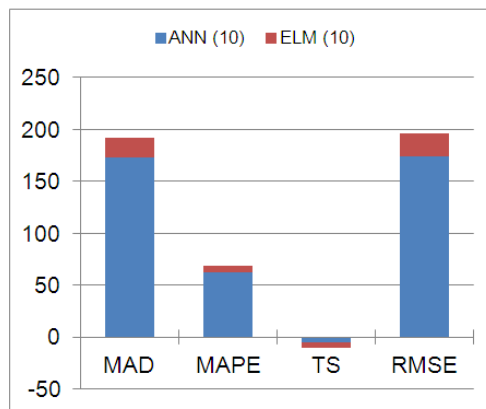
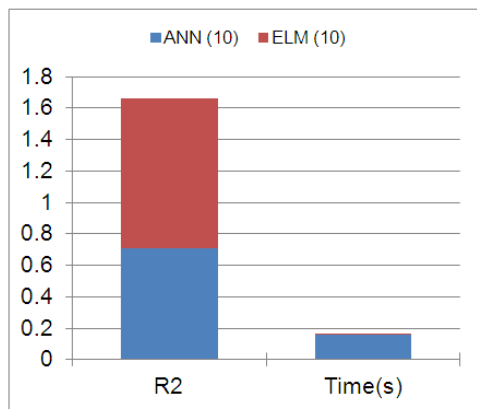
Figure 6: ANN and ELM Scatter Plots for Residual Stress Response at 10, 20 and 30 Nodes

Performance Metrics for Residual Stress at 10, 20 and 30 Nodes

The performance metrics for residual stress at 10, 20 and 30 nodes is shown in table 10.

Table 10: Performance Metrics for Residual Stress at 10, 20 and 30 Nodes

Metrics	ANN			ELM		
	10 Nodes	20 Nodes	30 Nodes	10 Nodes	20 Nodes	30 Nodes
MAD	143.28414	16.89536	19.30703	11.78426	5.02351	10.46137
MAPE	127.17983	16.31319	15.77781	9.84966	5.07485	10.18027
TS	-5	-5	-5	-5	-5	-5
R2	0.50933	0.72041	0.96519	0.75168	0.99032	0.99247
Time(s)	0.15784	0.08985	1.00246	0.00285	0.00089	0.00985
MSE	20954.24634	451.47165	483.50695	188.86352	50.02109	289.70185
RMSE	144.75582	21.24786	21.98879	13.74276	7.07256	17.02063



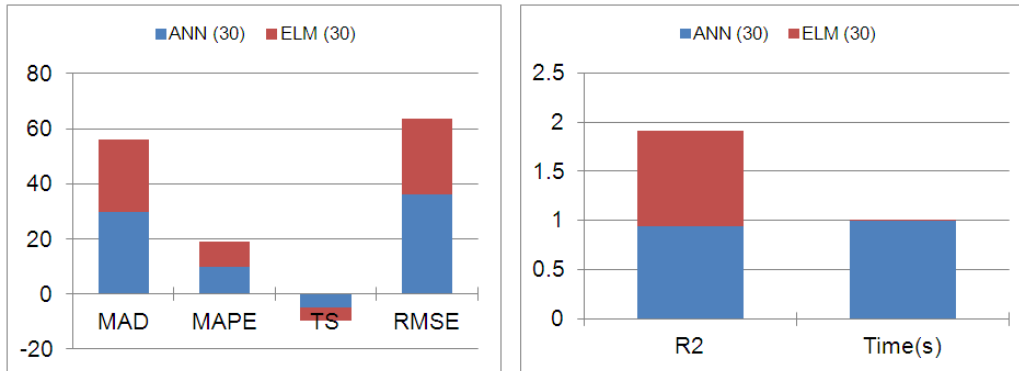


Figure 7: ANN and ELM Performance Metrics for Residual Stress at 10, 20 and 30 Nodes

III. Discussion Of Ann And Elm Results

The residual stress from the experimental data represents the target (expected) value while the output is the predicted value (response). The model was trained as the output neuron value was adjusted from 10 to 30 in the regression mode. The ELM model was verified against the ANN model which is one of the very popular machine learning black boxes. The ANN and ELM simulation results at 10 nodes, 20 nodes and 30 nodes alongside the experimental results are presented in Table 9. It can be seen from the table that the number of epochs and consequently the time needed for ANN and ELM modeling reduced with rise in the number of nodes. It is also seen from R^2 values and correlation that accuracy of ANN and ELM modeling improved with rise in number of nodes. This means that from both stand points of speed and accuracy, it is better to use higher number of nodes and lesser number of iterations than to use lower number of nodes and higher number of iterations.

Figure 5 show the graphical representation of the predicted values for tensile response at 10, 20 and 30 nodes for both ANN and ELM models. It can be observed from the graphs that at node 30, ELM was the same as the expected values at all the measured points. The advantages of the ELM over the classical ANN model are evident. For example, in accordance with the basic theory of ELM, randomly initiated hidden neurons are fixed, and they do not need iterative tuning process with free parameters or connections between hidden and output layer. Consequently, ELM is remarkably efficient to reach a global optimum, following universal approximation capability of single layer feed-forward network. With suitable activation functions, ELM can attain optimal generalization bounds of traditional feed forward neural networks in which all parameters are learned. This is a distinct advantage of the ELM model in terms of the efficiency and generalization performance over traditional learning algorithm such as ANN as revealed in this research.

Discussion of ANN and ELM Scatter Plots

The scatter plots of the predicted values at 10, 20 and 30 nodes are shown in figure 6. From the scatter plots of the predicted response, the highest degree of clusters at the linear regression line is clearly observed on the ELM model. This was specifically pronounced for the ELM model at 30 neural nodes. This particular statistical correlation of targeted and predicted responses at optimum of 30 nodes has a coefficient of determination (R^2) value of 99.2% for ELM, 96.5% for ANN and 92.4% for Taguchi robust design. This result shows that ELM has better prediction capability compared to ANN.

Discussion of Model Performance

Table 10 shows the performance metrics of ANN and ELM. The performances of the models were considered using results gotten from statistical metrics of equations 6 to 11. They are: Mean Square Error (MSE), Root Mean Square Error (RMSE), Mean Absolute Percentage Error (MAPE), Mean Absolute Deviation (MAD), Tracking Signal (TS), and Coefficient of Determination (R^2). Training time for each of the models was also recorded.

It is observed that ELM algorithm was simply magnificent in its training time which was much faster than ANN for all neural nodes. At 30 neural nodes, the training time for ELM was 0.009 Seconds while that of ANN was 1.00 Seconds.

The MSE and MAD are statistical approaches used to verify the prediction error. It was found that the MSE, RMSE, MAD and MAPE all improved as the output neuron value increased and fully converged at 30 neural nodes. This means that the higher the number of output neurons, the better the response. While the hidden nodes of ANN can be adjusted, they are not accessible in ELM.

The tracking signal (TS) helps to determine if the model is an accurate representation of the real-world variable. It is expected to be theoretically equal to zero. Both ELM and ANN models have tracking signals

recorded at sub-zero for all the nodes. This indicates that the models have good tracking signal; hence the models are good.

IV. Conclusions

At the end of this research, the following conclusions are made:

1. Based on analysis of the experimental results using Taguchi method, ANN and ELM algorithms, it can be concluded that all the methods gave reliable results.
2. Taguchi method can be successfully applied to optimize the process parameters that influence residual stress response of mild steel plate weldments whereas ANN and ELM models can be used for predicting the response.
3. By comparing the experimental results with those obtained using ANN and ELM models, it can be concluded that the ELM model is more efficient in predicting residual stress on mild steel plate weldments.

References

- [1]. Bate, S.K., Green, D. and Buttle, D. (1997). A review of residual stress distribution in welded joints for defect assessment of offshore structures. *Journal of Material Manufacturing and Processing*, 4(5), 28-36.
- [2]. Cullity, B.D. and Stock, S.R. (2001). *Elements of X-ray diffraction*. 1st ed. New Jersey: Prentice Hall.
- [3]. Cynthia, L. and Annette, O, 2004. *The metallurgy of steel*. American Welding Society. (9th edition). ISBN 9780871708588.
- [4]. Jain, R. K., 2013. *Production Technology*. Khanna Publishers (17th edition), New Delhi.
- [5]. Masubichi K. (1980). *Analysis of Welded Structures: Residual Stresses, Distortions and their Consequences*, Pergamon Press, Oxford, UK.
- [6]. Nasasimhan, J., Mcleavey, Z. and Billington, G., 1995. Composite function wavelength neural networks with extreme learning machine. *Journal of Neurocomputing*, 73(7), 1405-1416.
- [7]. Okafor, E.C., Ihueze, C. C. and Nwigbo, S.C., 2013. Optimization of hardness strengths response of plantain fibres reinforced polyester matrix composites applying Taguchi robust design. *International Journal of Engineering*, 26(1), 21-38.
- [8]. Rao, R.S., Ganesh, K.C., Shetty, P.S. and Phil, J.H., 2008. The Taguchi methodology as a statistical tool for biotechnological applications: A critical appraisal. *Biotechnology Journal*, 3(4), 510-523.
- [9]. Thorstom, H., 2017. Extreme learning machine and its applications. *Neural Computing and Applications*, 5, 14-34.
- [10]. Vonderembse, F. and White, T., 1991. Sales forecasting system based on gray Extreme Learning Machine with Taguchi method in retail industry. *Expert Systems with Applications*, 38(3), 1336-1345.
- [11]. Withers, P.J. and Bhadeshia, H.K. (2001). Residual stress: Part 1. *Journal of Material Science Technology*, 17, 355–365.